Journal of Instrumentation

PAPER • OPEN ACCESS

Cost-efficient single photon-sensitive nanosecond gated spectrometer based on commercial grade image intensifier

To cite this article: Patrik Ščajev and Algirdas Mekys 2023 *JINST* **18** P05026

Published by IOP Publishing for Sissa Medialab

Received: *March 6, 2023*
Revised: *April 14, 2023*
Accepted: *April 27, 2023*
Published: *May 22, 2023*

Cost-efficient single photon-sensitive nanosecond gated spectrometer based on commercial grade image intensifier

Patrik Ščajev* **and Algirdas Mekys**

Institute of Photonics and Nanotechnology, Vilnius University, Sauletekio al. 3, LT-10257, Vilnius, Lithuania

E-mail: patrik.scajev@ff.vu.lt

Abstract: A commercial grade low-cost image intensifier was modified with a fast transistor gating circuit for time-resolved photoluminescence spectra and decay measurements. Gating exposure of 20 ns and spectral sensitivity in the 300–1000 nm range were achieved. Operation frequency in 5 Hz to 0.3 MHz range was verified by a pulsed laser diode. Pulsed repetitive image detection was integrated on a cooled CMOS camera. High dynamic range and wide spectral resolution were achieved. The thermal noise, reduced by three orders of magnitude at −16°C cooling and a high gain of 10^4, allowed single photon detection. Application of the spectrometer for sensitive photoluminescence decay measurements at pulsed laser excitation was performed on $MAPbBr_3$ perovskite and CsI(Tl) scintillator crystals. The decay lifetimes of 400–600 ns and 100–6000 ns were determined, respectively. CsI(Tl) scintillator showed much stronger x-ray luminescence intensity due to larger defect density.

Keywords: Detectors for UV, visible and IR photons; Imaging spectroscopy; Optical sensory systems

*Corresponding author.

https://doi.org/10.1088/1748-0221/18/05/P05026

2023 JINST 18 P05026

Contents

1 **Introduction** 1

2 **Experimental setup** 2

3 **Results and discussion** 3

4 **Conclusions** 6

2023 JINST 18 P05026

1 Introduction

Time-resolved spectroscopy of organic and inorganic materials is of high importance for the improvement and development of optoelectronic devices and scintillators [1–6]. Typically, high repetition rate pulses are applied to the material and then photoluminescence (PL) spectra decays are monitored [7–9]. The intensity of PL and its decay time can be in wide ranges, thus needing a sensitive and complicated tool for its detection. The typically applied devices are streak cameras, photomultipliers, ICCD cameras. Streak cameras provide the best time resolution and wide dynamic range [10] but have the largest cost. Photomultipliers have time resolution limited to nanoseconds [11]. PL spectra can be obtained by scanning PL decays over wavelength using a motorized monochromator. The signal detection needs a fast oscilloscope. Thus the setup cost is increased by additional components. ICCD cameras [12] coupled to spectrometers provide similar time resolution as PMTs and have higher costs than PMTs but still by order magnitude lower than that of streak cameras. The signal readout is performed by inexpensive CMOS sensors. Compact ICCD spectrometers can be obtained using built in diffraction gratings for the whole visible spectral range. The core element of ICCD — image intensifier is widely produced for night vision devices and has very compact size. The scientific versions of the intensifiers have UV-enhanced photocathodes and gating electrodes. Intensifier is compact because of multichannel plate application having high photon gain and small size (typically 18 mm photocathode diameter). The intensifier's high spatial resolution, up to 74 lp/mm [13], allows full PL spectrum detection by projecting spectrometer output to the photocathode [14, 15]. Short electron transit time through the microchannel plate (MCP) allows fast gating of the device down to 100 picoseconds [16]. Nevertheless, commercial ICCDs use modified photocathodes with metal underlays for more rapid gating, and the signal is coupled by a fiber taper to the camera to reduce the device dimensions. On the other hand, this strongly increases the device costs.

In this work, we develop a cost-efficient analog of ICCD spectrometer using a commercial 18 mm image intensifier tube, relay lens and a standard CMOS camera. For proper device operation, the intensifier and camera are thermoelectrically cooled to −16°C to suppress the dark counts of the photocathode. The gating circuit is built using an ultrasonic transducer circuit architecture. Single photon sensitivity, nanosecond time resolution, sub-MHz operation were obtained. Testing of the device on a perovskite CsI(Tl) scintillator crystals revealed excitation-dependent photoluminescence spectra and decays.

2 Experimental setup

For cost-efficient spectrometer production, Gen. II+ CommGrade (S1100-I) Ø37 mm tube with image inversion was used. It had a P43 phosphor with 2 ms decay time, spatial resolution 66 lp/mm, input voltage 2–3.6 V, 6294 cd/m^2/lx luminance gain, external gain control (EGAC) function (by 50 times). The intensifier gating circuit and spectrometer construction are shown in figure 1. Flat-Field Concave Holographic Diffraction Grating blazed at 500 nm, 200 lines/mm UFC1 was obtained from DALIAN UNIQUE OPTICSCO., LTD. A cooled high dynamic range CMOS camera BFS-U3-63S4M-C coupled to the intensifier with a relay lens (F1.4) was used for amplified image detection. Thermoelectric cooling was obtained at −16°C with a 12 V two-stage thermoelectric cooler (TEC) with 50 W power and with an attached 10 × 10 × 10 cm processor aluminum heatsink with a 12 cm fan. The intensifier enclosure input and output windows were heated with SMD resistors to avoid condensation.

The gating circuit (figure 1(a)) consisted of a fast MOSFET transistor T1 (ARF463AP1G) with a driver IC1 (NCP81074B) to provide gate pulses replicating trigger pulses from the digital delay generator (Highland technology P400 digital delay and pulse generator), which was triggered by pulsed laser synchronization pulses. We modified the circuit design taken from [17, 18]. Intensifier was on when the −200 V pulses were provided to its photocathode, the other time, it was off by a constant 50 V voltage applied through resistor R9. The Zener diodes (D1, D2) were used for the transistor protection.

The spectrometer was tested on a $MAPbBr_3$ perovskite crystal by measuring its excitation-dependent PL spectra and decays using 10 ps, 10 Hz laser (EKSPLA) excitation at 1053 nm wavelength. The crystal production method and its properties are described in [19].

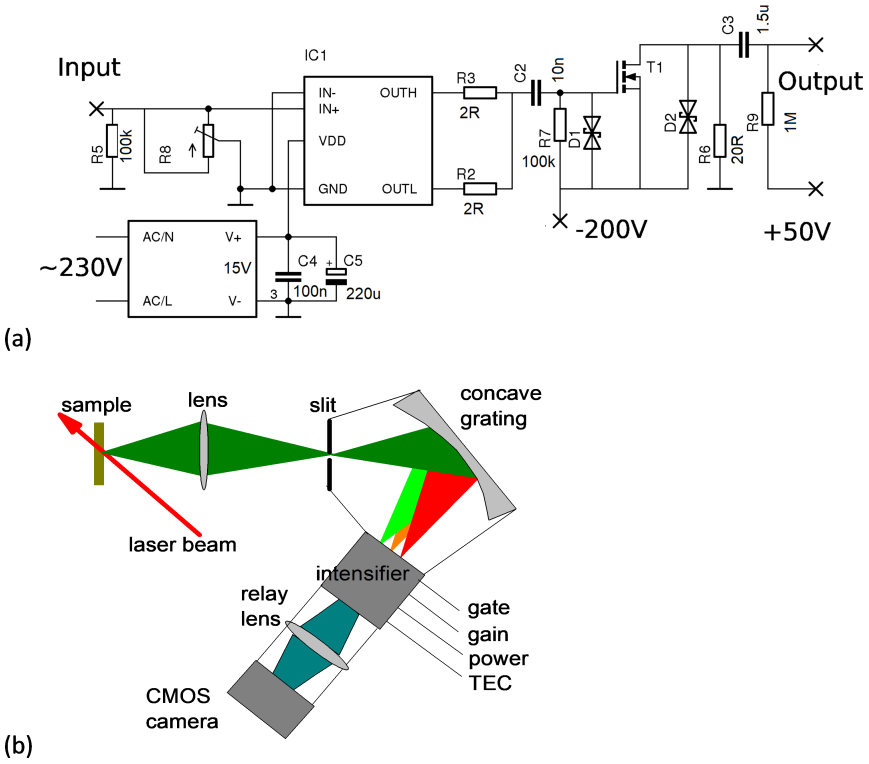

Figure 1. Image intensifier gating circuit (a) and intensified spectrometer schematic construction (b).

3 Results and discussion

Firstly, we tested the gating circuit. It provided 20 ns or longer pulses, as shown in figure 2(a). Therein, we show 20, 100, and 1000 ns gate pulses generated by a gating circuit using 12 V triggering pulses from the generator. Voltage transients were measured by Testec 1:100 300 MHz passive probe and 350 MHz Siglent oscilloscope. Negative voltage corresponds to gate open. Figure 2(b) shows the shortest gate and corresponding integrated intensifier response as measured delaying the gate pulses with respect to the short ten ps duration excitation laser pulse at 527 nm.

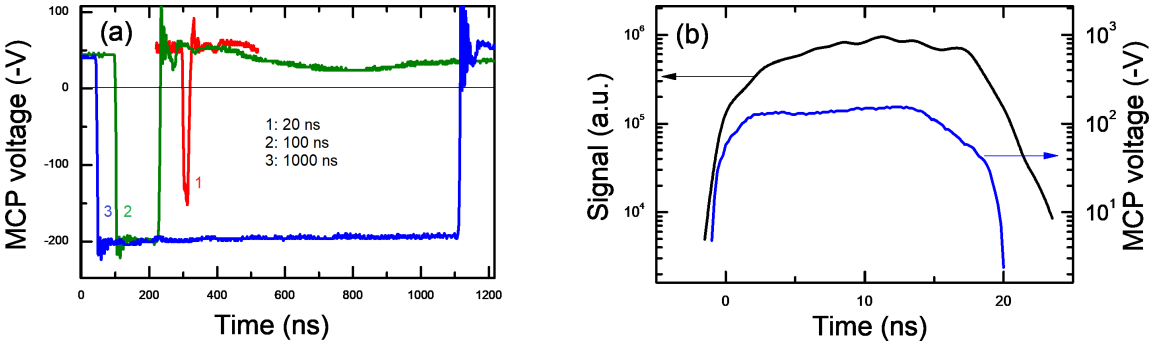

Figure 2. Different duration voltage gates (a) and short gate pulse correlation with integrated intensifier output (b).

Figure 3 shows detailed image intensifier output at different laser pulse delays. It is observed that the intensifier photocathode has parasitic resistivity and capacitance preventing its fast switch on. Full on-state is achieved at a 4 ns delay, while full off-state takes slightly larger time to achieve. The cooling strongly enhances the spectrometer operation. The number of thermal electrons generated in the photocathode at 24°C was 135000 e^-/s; at −16°C it reduced by three orders of magnitude to 180 e^-/s. Thus at a maximum 0.3 MHz operation frequency and at 20 ns gate duration, only one dark

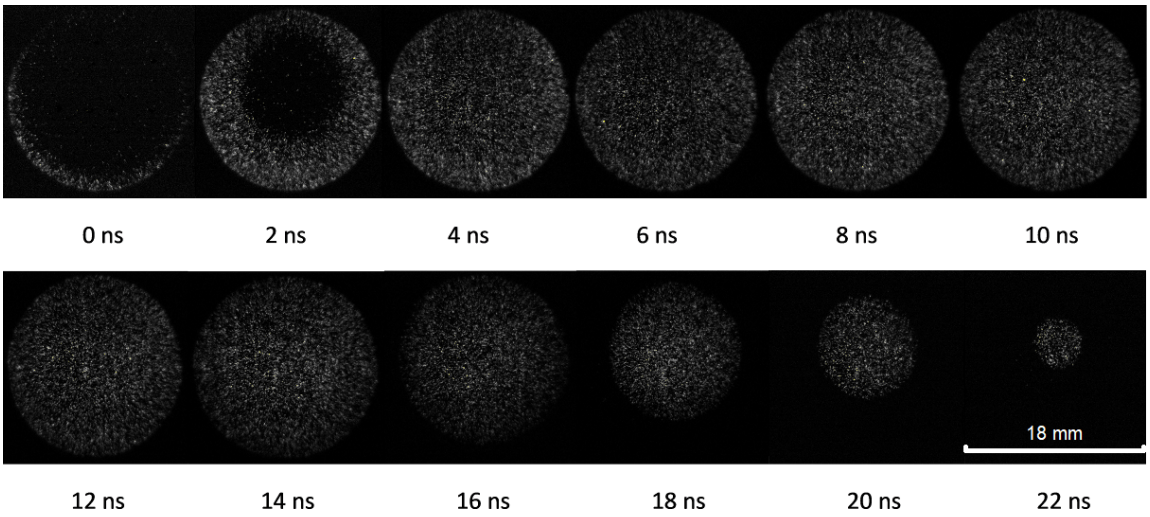

Figure 3. Images of intensifier output at different gate delays after ten ps duration pulse illumination. Voltage was applied from the bottom.

2023 JINST 18 P05026

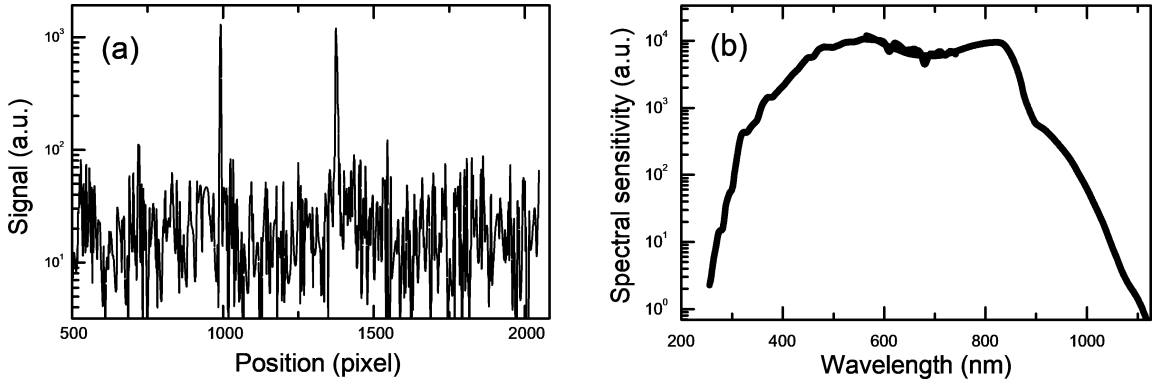

Figure 4. The resolution of single photons from the camera noise at 20 ns gate (a). The intensifier spectral sensitivity at −16°C temperature (b).

count per second appears. The single photon detection is shown in figure 4(a). Single photon peaks are well above the camera background and could lead to efficient low-level light detection. The spectrometer spectral response is shown in figure 4(b). It has the best response in the 300–1000 nm range (calculated at a 1 percent level from the responsivity maximum at 560 nm), where most light-emitting materials are investigated.

For the intensified spectrometer linearity investigation, regulated intensity laser pulses were used at 351 nm (figure 5). Intensifier response signal is almost linear vs. the excitation intensity, as observed in figure 5(b). Dynamic range of more than two orders of magnitude is achieved for fixed gain. Spectra broadening appears due to short laser pulse, grating, intensifier and relay lens spatial resolution [20] and the intensifier halo effect [21]. Spectral resolution was about one nm in FWHM.

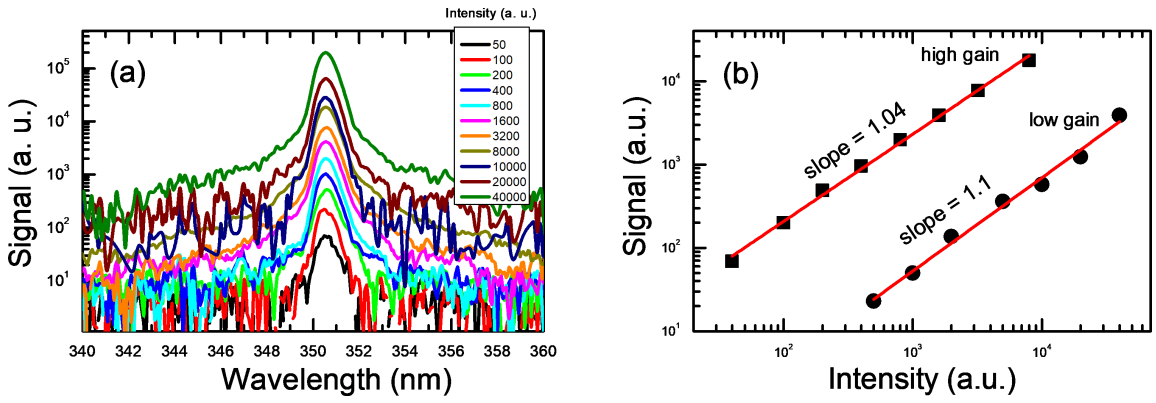

Figure 5. Intensifier response signal dependence on 351 nm laser pulse intensity (a). Signal linearity test at high and low gain (b). In (a) 3 upper curves correspond to high gain spectra shifted by gain coefficient of 49. Gate of 20 ns was applied.

The repetition rate impact on the spectrometer was tested using a pulsed laser diode (Picoquant D-C-420; 420 nm wavelength). Diode spectra at different repetition frequencies and diode electroluminescence intensity dependence of repetition frequency are shown in figure 6. At the highest frequencies calibrated filters were used to suppress laser pulse intensity. The spectrometer response is linear in a wide range, indicating proper gating operation. The gating circuit operates well up to

2023 JINST 18 P05026

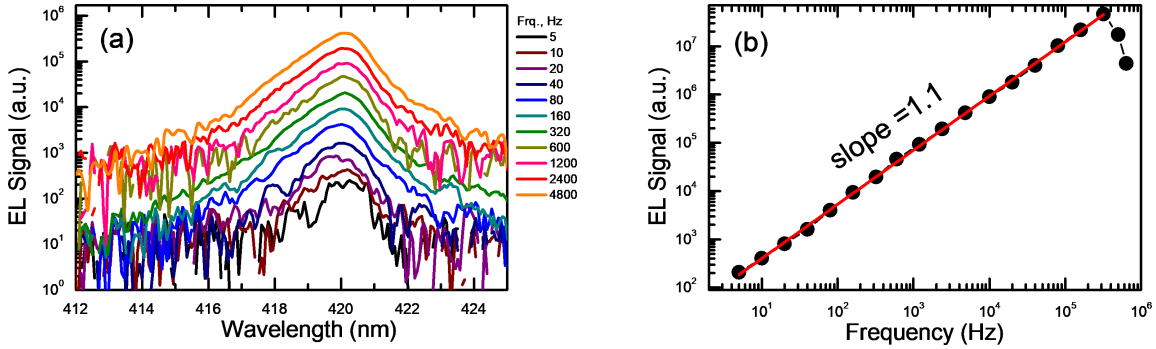

Figure 6. Response to pulsed laser excitation at different frequencies and 0.5 s camera integration (a), and response linearity vs. frequency (b). A gate of 20 ns was applied.

0.3 MHz, as circuit overload appears at higher frequencies. In comparison, ultrafast ICCD cameras have up to 1 MHz repetition rates [22].

In figure 7, we show the $MAPbBr_3$ perovskite crystal photoluminescence spectra and decays at different two-photon laser excitation intensities at 1053 nm (scattered excitation light was blocked by a filter). After the excitation pulses, the intensifier gate was delayed in a step manner to measure photoluminescence (PL) intensities at different delay times and reconstruct the PL decay. Here, two-photon excitation of the crystal is applied. Thus the PL signal depends on the excitation intensity by the 4^{th} power. While the PL signal depends as 2^{nd} power on the excited carrier density ΔN (i.e., PL $\sim \Delta N^2$). Almost single-exponential PL transients were observed with decay times in the 390–560 ns range. The spectra and decays well coincide with those obtained in [19], where a streak camera was applied for their measurements.

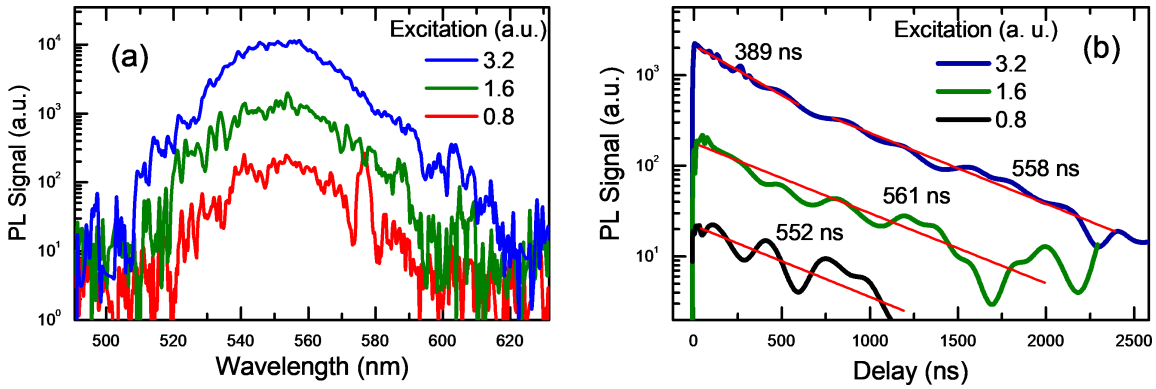

Figure 7. $MAPbBr_3$ perovskite crystal spectra (a) and decays (b) at different laser excitations at 1053 nm wavelength. Numbers in (b) show the determined exponential lifetimes.

In figure 8, we show CsI(Tl) scintillator x-ray luminescence (XL) spectra and CsI(Tl) photoluminescence decays excited at 351 nm wavelength. The PL spectra well coincide with the XL spectra indicating the same emission mechanism. The XL was generated by using x-ray tube 6cv27 with a massive Cu anode. The tube was powered with a regulated 30 kV power supply; 2.5 A cathode filament current was applied. The scintillator was placed on the spectrometer input slit opposite the x-ray tube Be output window. $MAPbBr_3$ perovskite nanocrystals can serve as cost-efficient

2023 JINST 18 P05026

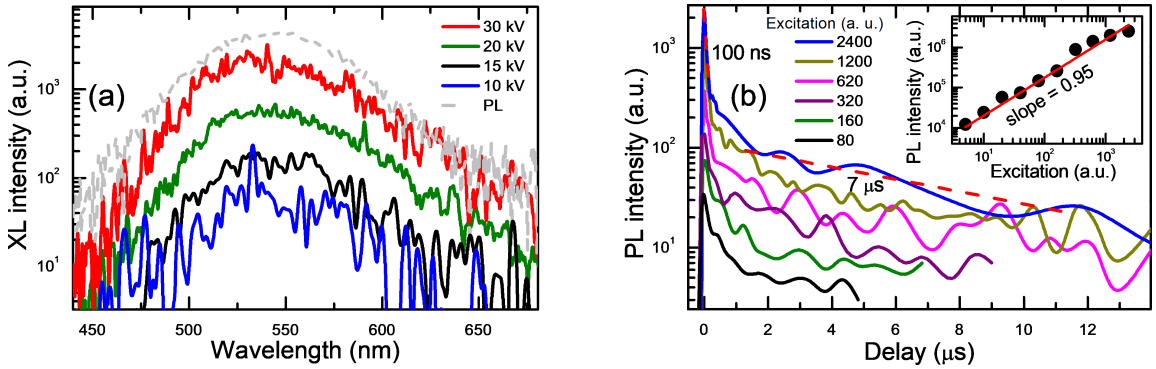

Figure 8. CsI(Tl) scintillator x-ray luminescence, PL spectra (a) and photoluminescence decays (b). Inset in (b) shows the integrated PL intensity dependence on the excitation intensity.

high-energy radiation detectors and scintillators for x-ray imagers [23]. Still in our perovskite $MAPbBr_3$ crystal, we did not observe XL even at 30 kV as it is 4400 times less efficient scintillator than CsI(Tl) [24]. This peculiarity can be explained by very low dopant and defect density in $MAPbBr_3$ encumbering XL at low carrier density x-rays can excite at applied conditions. On the other hand, the XL spectra intensity in CsI(Tl) scintillator increased with tube voltage due to the increasing intensity and energy of x-rays. The PL decays in CsI(Tl) were found non-exponential with fast (100 ns) and slow (7 µs) decay components [25]. The integral PL signal amplitude was linear on the excitation intensity (i.e., PL $\sim \Delta N$), indicating that the defect emission regime is dominant [25, 26].

To sum up, the developed spectrometer shows 300–1000 nm spectral sensitivity interval, 1.2 nm spectral resolution, 300 kHz operating frequency, and 20 ns minimal gate duration. The materials costs for the spectrometer were around 3000 EUR. For comparison, the Andor iStar sCMOS camera with sCMOS sensor can operate in the 180–920 nm range, at maximum 500 kHz frequency, has a P43 phosphor (2 ms), 18 mm image intensifier, and < 50 ns gate. The camera price is 52000 EUR. Compact spectrometer-monochromator CS130B-1-FH with 130 mm focal length, suitable for the camera spectral range, has a price of 8718 EUR [27]. With the camera, the spectral resolution of about 1.6 nm for 1000 nm spectral band-pass can be achieved. Therefore, the developed spectrometer cost is more than an order of magnitude lower than that of the existing commercial devices and can be broadly used for various semiconductor characterization and radiation detection by scintillators.

4 Conclusions

We developed a cost-efficient single photon-sensitive nanosecond gated spectrometer based on a commercial grade image intensifier. Gate durations down to 20 ns, repetition rates up to 0.3 MHz, and spectral range of 300-1000 nm were achieved. Testing of the gated spectrometer on $MAPbBr_3$ perovskite and CsI(Tl) scintillator crystals allowed to efficiently measure their photoluminescence spectra and decays indistinguishable from commercial high-cost gated spectrometers. This device opens the perspective for economic applications in testing of scintillators and semiconductor materials for optoelectronic mass production devices.

2023 JINST 18 P05026

Declaration of competing interest. The authors declare that they have no known competing financial interests or personal relationships that could have appeared to influence the work reported in this paper.

Data availability. Data will be made available on request.

Acknowledgments

The research was supported by the Research Council of Lithuania under the project No. S-MIP-19-34.

References

[1] D. Sirbu, F.H. Balogun, R.L. Milot and P. Docampo, *Layered perovskites in solar cells: Structure, optoelectronic properties, and device design*, *Adv. Energy Mater.* **11** (2021) 2003877.

[2] A. Bercegol, G. El-Hajje, D. Ory and L. Lombez, *Determination of transport properties in optoelectronic devices by time-resolved fluorescence imaging*, *J. Appl. Phys.* **122** (2017) 203102.

[3] A. Bercegol, J. Mellado, A. Rebai, J. Rousset, D. Ory and L. Lombez, *Determination of transport properties in optoelectronic devices by time-resolved fluorescence imaging*, *Proc. SPIE* **10527** (2018) 1052704.

[4] X.-B. Wang, L.-L. Yan, Y. Li and X.-J. Li, *Time-Resolved Photoluminescence Study of Silicon Nanoporous Pillar Array*, *Chin. Phys. Lett.* **32** (2015) 097802.

[5] A. Aamoum, K. Waszkowska, S. Taboukhat, P. Płóciennik, M. Bakasse, Y. Boughaleb et al., *Time-resolved photoluminescence and optical properties of a specific organic azo dye*, *Opt. Quantum Electron.* **52** (2019) 35.

[6] P. Ščajev, R. Durena, P. Onufrijevs, S. Miasojedovas, T. Malinauskas, S. Stanionyte et al., *Morphological and optical property study of Li doped ZnO produced by microwave-assisted solvothermal synthesis*, *Mater. Sci. Semicond. Process.* **135** (2021) 106069.

[7] E.P. Farr, J.C. Quintana, V. Reynoso, J.D. Ruberry, W.R. Shin and K.R. Swartz, *Introduction to time-resolved spectroscopy: Nanosecond transient absorption and time-resolved fluorescence of Eosin B*, *J. Chem. Educ.* **95** (2018) 864.

[8] H. Yan, X. Liang, S. Dong, Y. Lei, G. Zhang, R. Chen et al., *Exploration of exciton dynamics in GaTe nanoflakes via temperature- and power-dependent time-resolved photoluminescence spectra*, *Opt. Express* **29** (2021) 8880.

[9] P. Ščajev, S. Miasojedovas, A. Mekys, D. Kuciauskas, K.G. Lynn, S.K. Swain et al., *Excitation-dependent carrier lifetime and diffusion length in bulk CdTe determined by time-resolved optical pump-probe techniques*, *J. Appl. Phys.* **123** (2018) 025704.

[10] https://www.azooptics.com/optics-equipment-details.aspx?EquipID=1059.

[11] N. Matsunaga et al., eds., *Photomultiplier tubes, Basics and applications*, fourth edition, Hamamatsu Photonics K.K. (2017).

[12] https://www.photek.com/icoms-160/.

[13] https://alpha-photonics.com/produkt/commgrade-echo-zw0124-ag-o37mm/?lang=en.

[14] V. Protopopov, *A Compact Wide-Range Spectrometer with Image Intensifier: Unexpected Advantages, New Functions, and a Variety of Applications*, *Appl. Spectrosc.* **66** (2012) 496.

2023 JINST 18 P05026

[15] Y. Fang, M. Zhang, J. Wang, L. Guo, X. Liu, Y. Lu et al., *A four-channel ICCD framing camera with nanosecond temporal resolution and high spatial resolution*, *J. Mod. Opt.* **68** (2021) 661.

[16] H. Sparks, F. Görlitz, D.J. Kelly, S.C. Warren, P.A. Kellett, E. Garcia et al., *Characterisation of new gated optical image intensifiers for fluorescence lifetime imaging*, *Rev. Sci. Instrum.* **88** (2017) 013707.

[17] J. Brown and G. Lockwood, *Low-cost, high-performance pulse generator for ultrasound imaging*, *IEEE Trans. Ultrason., Ferroelect., Freq. Contr.* **49** (2002) 848.

[18] Y. Fang, Y. Gou, M. Zhang, J. Wang and J. Tian, *A MOSFET-based high voltage nanosecond pulse module for the gating of proximity-focused microchannel plate image-intensifier*, *Nucl. Instrum. Meth. A* **987** (2021) 164799.

[19] P. Ščajev, S. Miasojedovas and S. Juršėnas, *A carrier density dependent diffusion coefficient, recombination rate and diffusion length in $MAPbI_3$ and $MAPbBr_3$ crystals measured under one- and two-photon excitations*, *J. Mater. Chem. C* **8** (2020) 10290.

[20] D.M. Devia, L.V. Rodriguez-Restrepo and E. Restrepo-Parra, *Methods employed in optical emission spectroscopy analysis: a review*, *Ing. Cienc.* **11** (2015) 239.

[21] D. Cui, L. Ren, F. Shi, J. Shi, Y. Qian, H. Wang et al., *Test and analysis of the halo in low-light-level image intensifiers*, *Chin. Opt. Lett.* **10** (2012) 060401.

[22] L. Cester, A. Lyons, M.C. Braidotti and D. Faccio, *Time-of-Flight Imaging at 10 ps Resolution with an ICCD Camera*, *Sensors* **19** (2019) 180.

[23] A. Jana, S. Cho, S.A. Patil, A. Meena, Y. Jo, V.G. Sree et al., *Perovskite: Scintillators, direct detectors, and x-ray imagers*, *Mater. Today* **55** (2022) 110.

[24] H. Yu, X. Meng, S. Yang, J. Zhao, X. Zhen and R. Tai, *Photonic-crystals-based GAGG:Ce scintillator with high light output and fast decay time for soft x-ray detection*, *Nucl. Instrum. Meth. A* **1032** (2022) 166653.

[25] V.B. Mikhailik, V. Kapustyanyk, V. Tsybulskyi, V. Rudyk and H. Kraus, *Luminescence and scintillation properties of CsI — a potential cryogenic scintillator*, *Phys. Stat. Sol. B* **252** (2015) 804 [arXiv:1411.6246].

[26] P. Sintham, P. Saengkaew and S. Sanorpim, *Optical properties of CsI:Tl crystals grown using different precursors purities*, *J. Phys. Conf. Ser.* **1144** (2018) 012105.

[27] https://www.newport.com.

2023 JINST 18 P05026